

Current carrying capacity of carbon nanotubes

M. P. Anantram

NASA Ames Research Center, Mail Stop T27A-1, Moffett Field, CA, USA 94035-1000

Abstract

The current carrying capacity of ballistic electrons in carbon nanotubes that are coupled to ideal contacts is analyzed. At small applied voltages, where electrons are injected only into crossing subbands, the differential conductance is $4e^2/h$. At applied voltages larger than $\Delta E_{NC}/2e$ (ΔE_{NC} is the energy level spacing of first non crossing subbands), electrons are injected into non crossing subbands. The contribution of these electrons to current is determined by the competing processes of Bragg reflection and Zener type inter subband tunneling. In small diameter nanotubes, Bragg reflection dominates, and the maximum differential conductance is comparable to $4e^2/h$. Inter subband Zener tunneling can be non negligible as the nanotube diameter increases because ΔE_{NC} is inversely proportional to the diameter. As a result, with increasing nanotube diameter, the differential conductance becomes larger than $4e^2/h$, though not comparable to the large number of subbands into which electrons are injected from the contacts. These results may be relevant to recent experiments in large diameter multi-wall nanotubes that observed conductances larger than $4e^2/h$.

Journal Reference: Phys. Rev. B, vol. 62, p. 4837, (2000)

Introduction: Most experimental¹⁻³ and theoretical work of electron transport in individual nanotubes deals with single wall nanotubes (SWNT). In these experiments, the spacing between subbands is typically larger than the applied voltage and thermal energy kT . Recent experiments on multi-wall nanotubes (MWNT)⁴⁻⁶ are fundamentally different in that the subband spacing is comparable to the applied voltage and only a few times larger than the room temperature kT . It is further believed that transport in these experiments primarily takes place along individual layers, with little inter-layer coupling. From the view point of molecular electronics, the relatively small low bias resistance of 500Ω in multi-wall nanotube wires reported in Ref. 6 is very promising. In addition, Ref. 4 found that the increase in differential conductance with applied voltage was not commensurate with the increase in number of subbands in large diameter nanotubes. On the theoretical side, Ref. 7 found long tails in the screening properties of metallic nanotubes. Motivated by the above work, we study the current carrying capacity of electrons injected into a nanotube by including the non crossing subbands.

Central idea and basic processes involved: The central idea of this paper is that an applied bias across the nanotube results in a *transport bottle neck* due to Bragg reflection. This results in a smaller than expected increase in differential conductance with increase in applied bias.

In a defect free nanotube connected to ideal contacts, there are three possibilities for an electron injected from the left contact (Fig. 1): (i) Direct transmission, where an electron is transmitted in the injected subband (solid line of Fig. 1), (ii) Bragg reflection, which occurs when the wavevector (k) of an injected electron evolves to a value where the velocity in subband n , $v_n(k) = \frac{1}{\hbar} \frac{dE_n(k)}{dk} = 0$ (subband extrema). In Fig. 1, an electron injected from the left contact into a non crossing subband undergoes Bragg reflection at the location of the arrow (dotted line), and (iii) Inter subband Zener type tunneling, which involves tunneling between subbands induced by an electric field. The spacing between non crossing subbands (ΔE_{NC} of Fig. 1) decreases inversely with increase in nanotube diameter (D), $\Delta E_{NC} \propto 1/D$. So, we surmise that Zener tunneling becomes increasingly important in

determining the I-V curve with increase in nanotube diameter. The relative importance of these three phenomena depends on the energy, potential profile, and nanotube diameter, as discussed in this paper.

Method: The current is computed using the Landauer-Buttiker formula,

$$I = \int dE T(E) [f_L(E) - f_R(E)] , \quad (1)$$

where, $T(E)$ is the total transmission (single particle transmission probability summed over all subbands), and $f_L(E)$ and $f_R(E)$ are the Fermi factors in the left (μ_L) and right (μ_R) contacts respectively. We calculate the total transmission within the context of the pi-orbital approximation, where the hopping parameter is assumed to be 3.1 V. The method to calculate the total transmission is the same as in Ref. 8. The calculation of the I-V curve requires the potential drop across the nanotube. The potential drop should in principle be determined by the self-consistent solution of Poisson's equation and the non equilibrium electron density. This is a difficult problem for nanostructures. So, to convey the essential physics illustrating the role of Zener tunneling, we assume analytical profiles to simulate different values of the electric field, as discussed below. Finally, the nanotube is assumed to be coupled to ideal contacts, which means semi-infinite nanotube leads. So a work function mismatch between the nanotube and real contacts, and the accompanying electrostatics is neglected.

Results: The total transmission (and hence current) is determined by two physical parameters:

(i) ΔE_{NC} , the energy level spacing between the first non crossing subbands (Fig. 1). ΔE_{NC} depends on diameter, and for a (N,N) nanotube,

$$\Delta E_{NC} = 2t_0 \sin\left(\frac{\pi}{N}\right) , \quad (2)$$

where, t_0 is the hopping parameter between nearest neighbor carbon atoms. At applied voltages smaller than $\Delta E_{NC}/2e$, there is net injection of electrons only into the two crossing subbands. When the applied voltage is larger than $\Delta E_{NC}/2e$, electrons are injected into

the non crossing subbands. The electrons injected into the non crossing subbands can in principle contribute to current only if final states into which they can be transmitted are available. As can be seen from Fig. 1, when $V_a \geq \Delta E_{NC}/e$, electrons incident into the first non crossing subband below the band center (in the left contact) can tunnel into states of the first non crossing subband above the band center (in the right contact). $\Delta E_{NC}/e$ is the equivalent of the barrier height for this tunneling process.

(ii) The length over which an applied bias drops. This corresponds to the barrier length [the distance across which an electron should tunnel to reach a right moving state (Fig. 1)] for electrons injected into the first non crossing subband.

As ΔE_{NC} varies with diameter, we consider nanotubes with diameters varying from 6.8Å to 27.2 Å. They are the (5,5) [3.64eV], (10,10) [1.92eV], (13,13) [1.48eV], (16,16) [1.22 eV] and (20,20) [0.98 eV] nanotubes (ΔE_{NC} is given in the square brackets). The barrier length (and so the electric field) is varied by considering the potential to drop linearly in sections that are 10Å, 30Å and 60Å long. We have also calculated the effect of Zener tunneling by taking the applied potential (V_a) to drop across the nanotube as,

$$V(x) = \frac{V_a}{2} \left\{ 1 + \frac{1 + e^{\frac{L_t}{L_{sc}}}}{e^{\frac{L_t}{L_{sc}}} - e^{-\frac{L_t}{L_{sc}}}} e^{-\frac{x}{L_{sc}}} - \frac{1 + e^{-\frac{L_t}{L_{sc}}}}{e^{\frac{L_t}{L_{sc}}} - e^{-\frac{L_t}{L_{sc}}}} e^{\frac{x}{L_{sc}}} \right\}, \quad (3)$$

where, L_t is the length of the nanotube, and a typical value of $L_t=2500\text{Å}$. L_{sc} is a parameter that determines the nature of the voltage drop and x is the nanotube axis. $L_{sc} > L$ corresponds to a linear voltage drop. $L_{sc} < L$ corresponds to a scenario with large potential drops near the left and right ends, and a flat potential in between. As a result, for an applied voltage, the maximum electric field is smaller when Eq. (3) is used instead of a linear potential drop. As a result of this the Zener tunneling strength is smaller than in the linear case, and the total transmission versus energy has a different form. There is however no significant qualitative change of the main points discussed in the paper when Eq. (3) is used.

The results for the 60Å case is discussed first. At applied voltages smaller than $\Delta E_{NC}/2e$, there is net injection of electrons only into the two crossing subbands. As a result, the I-V

curve is linear, with the differential conductance equal to $4e^2/h$ [Fig. 2]. This is true more or less independent of the distance over which the voltage drops. For $V_a > \Delta E_{NC}/2e$, electrons are injected into the higher subbands. Yet the maximum differential conductance in Fig. 2(a) is approximately $4e^2/h$. This is because electrons injected in the non crossing subbands are primarily reflected, and so do not carry an appreciable current. To see this more clearly, consider the case of $V_a = 2.5V$. Here, electrons are injected from the left into twenty subbands. In Fig. 3, we show that for the 60\AA case, all non crossing subbands (solid and dotted lines) are almost fully Bragg reflected, and the crossing subbands are fully transmitted. Hence, the maximum differential conductance in Fig. 2(a) is approximately equal to $4e^2/h$. Alternately, electrons incident in the *non-crossing* subbands have to traverse a spatial region with only the *crossing* subbands, before tunneling into the right contact. Hence, in the absence of significant inter subband tunneling, they are reflected. The above picture changes at voltages above $3.1V$, which corresponds to a subband extrema of the crossing subbands. When $V_a > 3.1V$, there is almost no increase in current with applied voltage, in the voltage regime considered. This regime is explained by using $V_a = 3.5V$ [Fig. 4]. When $V_a = 3.5V$, electrons are injected into thirty five subbands from the left contact at $E = -V_a$. However, in a small energy range near $E = 0$ and $-V_a$, the total transmission is approximately one. This is because electrons injected into one of the two crossing subbands near $E=0$ are Bragg reflected (at $E=0$, only one of the two crossing subbands has a right moving state in the right contact). Similarly, near $E = \mu_L$, only one crossing subband has a right moving state at the left contact. In between these energy windows with unity total transmission, both crossing subbands are transmitted. The electrons injected into the non crossing subbands are almost fully Bragg reflected as discussed in the case of $V_a = 2.5V$. Upon increasing the applied voltage, the energy ranges where a single crossing subband carries current broadens, and the central energy range in between where both crossing subbands carry current [Fig. 3] becomes narrower. The current, which is approximately the integral of the area under the curve between $E=0$ and $-V_a$ does not increase much with further applied voltage as shown in Fig. 2. The explanation for the other nanotubes in Fig. 2(a) is no different except that

the larger value of the barrier height ΔE_{NC} makes Bragg reflection only more important when compared to the (20,20) nanotube.

The I-V characteristics in Fig. 2(a) were primarily determined by the crossing subbands because all other subbands are almost completely Bragg reflected. This picture changes when inter subband Zener tunneling or defect induced inter subband scattering are non negligible. To elucidate their effect on the I-V curve, we study their effects independently.

Zener tunneling, in principle begins to occur when $V_a = \Delta E_{NC}/e$ [Fig. 1]. At this voltage, electrons incident in the first non crossing subband below $E=0$ (in the left contact) are able to tunnel into states of the first non crossing subband above $E=0$ (in the right contact), as shown in Fig. 1. $\Delta E_{NC}/e$, which is the barrier height decreases inversely with increase in nanotube diameter [the diameter is directly proportional to N for a (N,N) nanotube], $\Delta E_{NC} \propto 1/N$ [Eqn. (1)]. So, we expect Zener tunneling to become more important with increase in nanotube diameter. Figs. 2 (b) and (c) shows that the calculated I-V deviates significantly from Fig. 2(a) as a result of inter subband Zener tunneling. The main points are that Zener tunneling and hence deviation of current from Fig. 2(a) increases, (i) at smaller applied voltages, as the nanotube diameter increases and the corresponding barrier height decreases [Figs. 2(b) and (c)], and (ii) with increasing electric field [Figs. 2(a)-(c)] as the distance over which an electron has to tunnel is smaller. A plot of the total transmission versus energy throws further light on the physics involved. When the bias drops over 30\AA , the opening and closing of a transmission window due to the first non crossing subband (solid line marked NC1) is at energies of about 0.5eV and 2.0eV respectively. These energies correspond to $\Delta E_{NC}/2$ below (0.5eV) and above (2.0eV) the nanotube band centers near the left and right contacts respectively. In the case of $L=10\text{\AA}$, the opening and closing of a second transmission window due to the second non crossing subband (dotted line marked NC2) at energies of about 1eV and 1.5eV respectively is seen. Also, the transmission probability of NC1 is larger in comparison to the 30\AA case because of the smaller barrier length. While the differential conductance at $V_a = 2.5V$ is not comparable to the twenty injected subbands, the contribution to current due to Zener tunneling cannot be neglected.

Frank et. al reported a constant conductance for applied voltages smaller than an estimate of $\Delta E_{NC}/e$ for their large diameter nanotubes, and a modest increase in conductance with applied bias for larger applied voltages.⁴ This increase in conductance did not reflect the large increase in the number of subbands with bias. The transport bottle neck discussed in this paper offers a possible physical mechanism that qualitatively explains the small increase in conductance with applied voltage in Ref. 4.

Finally, we discuss the role of defect assisted inter subband scattering. From a physical view point, Bragg reflection is weakened because defect scattering produces a non zero probability for an electron incident in a non crossing subband to reach the right contact, by scattering into right moving states of other subbands. To model defects, we follow section IIIA of Ref. 8, where the on-site potential is varied randomly. We consider a 2500Å long nanotube section with defects, and the applied voltage drops linearly. So, Zener tunneling is not important here, and all inter subband tunneling is defect induced. The I-V curve is shown for two different strengths of defect scattering in Fig. 5. The numbers in the legend correspond to ϵ_{random} of Ref. 8, and a larger value corresponds to larger defect scattering. In Fig. 5, at small voltages, only the crossing subbands determine the physics. Hence, the reflection of electrons in the crossing subbands causes a diminished current and differential conductance in comparison to the defect free case. At higher applied voltages, the differential conductance is larger than in the defect free case because the non crossing subbands are partially transmitted. Transmission of electrons incident in the non crossing subbands is illustrated in the inset of Fig. 5, which is a plot of total transmission versus energy with and without defect scattering ($\epsilon_{random} = 0.25eV$) at $V_a = 4V$, for $-V_a < E < 0$. Defect scattering enhances the total transmission near $E = 0$ and $-V_a$ to values larger the defect free case. Thus showing that electrons injected in the crossing subbands are transmitted in non crossing subbands at the right end (inset of Fig. 5).

While both Zener tunneling and defect scattering enhance the differential conductance at large applied voltages, the following features differentiate them. At biases smaller than $\Delta E_{NC}/e$, defects cause a reduction in current in comparison to the Zener tunneling case,

which continues to yield a conductance of $4e^2/h$. At biases larger than $\Delta E_{NC}/e$ electrons are injected into many subbands. The differential conductance in the case of Zener tunneling is larger than $4e^2/h$. Defect scattering alone, on the other hand, produces a differential conductance that is smaller than $4e^2/h$. This is because electrons incident in the *non-crossing* subbands have to traverse a spatial region where only the *crossing* subbands are present, before being transmitted to the right contact.

In conclusion, we have investigated the current carrying capacity of carbon nanotubes by including transport through non crossing subbands. This study considered ballistic transport and neglected electron-phonon interaction.⁹ We showed that due to the unique band structure of carbon nanotubes, Bragg reflection of electrons incident in the non crossing subbands is an important mechanism for the reduction of differential conductance. The differential conductance of nanotubes will be diameter dependent from purely ballistic processes due to competition between Bragg reflection and Zener type inter subband tunneling. The importance of Zener tunneling was studied by varying both the nanotube diameter and the length over which the voltage drops. The barrier height for Zener tunneling is equal to the inter subband energy level spacing ΔE_{NC} of Fig. 1, which decreases inversely with increase in nanotube diameter. As a consequence, for small diameter nanotubes, the differential conductance cannot be larger than $4e^2/h$ for voltages smaller than 3.1V, and is close to zero at larger applied voltages. Zener tunneling becomes more important with increasing nanotube diameter because $\Delta E_{NC} \propto 1/\text{Diameter}$. Also, Zener tunneling is stronger when the voltage drops across a smaller length. We show for increasing nanotube diameter, the total transmission is not negligible in certain energy windows, where the non crossing subbands carry current [Fig. 3]. As a result, the differential conductance at biases larger than $\Delta E_{NC}/e$ is larger than $4e^2/h$ [Fig. 2]. It should be emphasized that the differential conductance is however not comparable to the large number of subbands into which electrons are injected from the contacts. The role of defect scattering in the absence of Zener tunneling is also discussed. It is shown that at biases smaller than 3.1V, defect scattering leads to a differential conductance that is smaller than $4e^2/h$. For biases larger than 3.1 V, defects

increase the differential conductance when compared to the defect free case.

Useful discussions with Zhen Yao, Cees Dekker, T. R. Govindan, Adrian Batchold and Walt de Heer are acknowledged. I would like to thank Bryan Biegel for correcting an earlier version of the manuscript and discussions.

REFERENCES

- ¹ S. J. Tans, M. Devoret, H. Dai, A. Thess, R.E. Smalley, L.J. Geerligs and C. Dekker, Nature **386**, 474 (1997).
- ² D. H. Cobden, M. Bockrath, P. L. McEuen, A. G. Rinzler and R. E. Smalley, Spin Splitting and Even-Odd Effects in Carbon Nanotubes Phys. Rev. Lett **81**, 681 (1998)
- ³ H. T. Soh, A. F. Morpurgo, J. Kong, C. M. Marcus, C. F. Quate and H. Dai, Preprint (1999).
- ⁴ S. Frank, P. Poncharal, Z. L. Wang and W. A. de Heer, Science **280**, 1744 (1998); P. Poncharal, S. Frank, Z. L. Wang and W. A. de Heer, Preprint
- ⁵ C. Schonenberger, A. Bachtold, C. Strunk, J.-P. Salvetat and L. Forro, Interference and Interaction in Multiwall Carbon Nanotubes, cond-mat/9905144
- ⁶ P. J. de Pablo, E. Graugnard, B. Walsh, R. P. Andres, S. Datta and R. Reifenberger, Appl. Phys. Lett. **74**, 323 (1999)
- ⁷ M. F. Lin and D. S. Chuu Phys. Rev. B, **56**, 4996 (1997);
- ⁸ M. P. Anantram and T. R. Govindan, Phys. Rev. B **58**, 4882 (1998); M. P. Anantram, Jie Han and T. R. Govindan, Conference proceedings: Annals New York Academy of Sciences and Technology, **852**, 169 (1998)
- ⁹ Z. Yao, C. L. Kane and C. Dekker, Phys. Rev. Lett., **84**, 2941 (2000)

Figure Captions:

Fig. 1: Each rectangular box is a plot of energy versus wavevector, with the subband bottom equal to the electrostatic potential. Only a few subbands are shown for the sake of clarity. The three processes shown are direct transmission (solid line), Bragg reflection (dotted line) and inter subband Zener tunneling (dashed line).

Fig. 2: Current versus applied voltage for three different lengths across which the applied voltage drops, (a) 60 Å, (b) 30 Å, and (c) 10 Å. The results for tubes with five different diameters are shown. Zener tunneling is negligible in (a). For a given nanotube, the importance of Zener tunneling increases with increase in the electric field strength, as in (b) and (c). For a given applied voltage, the importance of Zener tunneling increases with increase in nanotube diameter.

Fig. 3: The left and right columns are the nanotube band structure close to the left and right contacts respectively. The central column is the total transmission versus energy for three different lengths (60Å, 30Å and 10Å) over which the voltage drops. The current (Fig. 2) is the integral of the total transmission from μ_R to μ_L . The Zener tunneling probability is negligible for the non crossing subbands in the case of $L=60\text{\AA}$. For $L=30\text{\AA}$ and 10\AA , the opening and closing of a transmission window due to the first non crossing subband (solid line marked NC1) is seen. For $L=10\text{\AA}$, the opening and closing of a transmission window due to the second non crossing subband (dotted line marked NC2) is also seen. $V_a = 2.5\text{V}$.

Fig. 4: The total transmission versus energy for $V_a = 3.5\text{V}$. The total transmission is equal to one in energy ranges near the band centers in the left and right contacts, where crossing subbands are absent at either the left or right ends. The total transmission in between is approximately two, corresponding to transmission of both crossing subbands.

Fig. 5: Current versus applied voltage for a (10,10) nanotube in the presence of defects. For $V_a < 3.1\text{V}$, the differential conductance decreases with increase in the defect scattering strength. For $V_a > 3.1\text{V}$, the differential conductance with defects is larger than the defects free case. This is because inter subband scattering opens channels for transport involving the non crossing subbands. The strength of defect scattering increases with increase in ϵ_{random} .

Inset: Total transmission versus energy with and without defect scattering, when $V_a = 4V$,
Note that in comparison to the defects free case, the total transmission is larger than one in
energy windows near 0 and $-V_a$.

Fig. 1 / Anantram

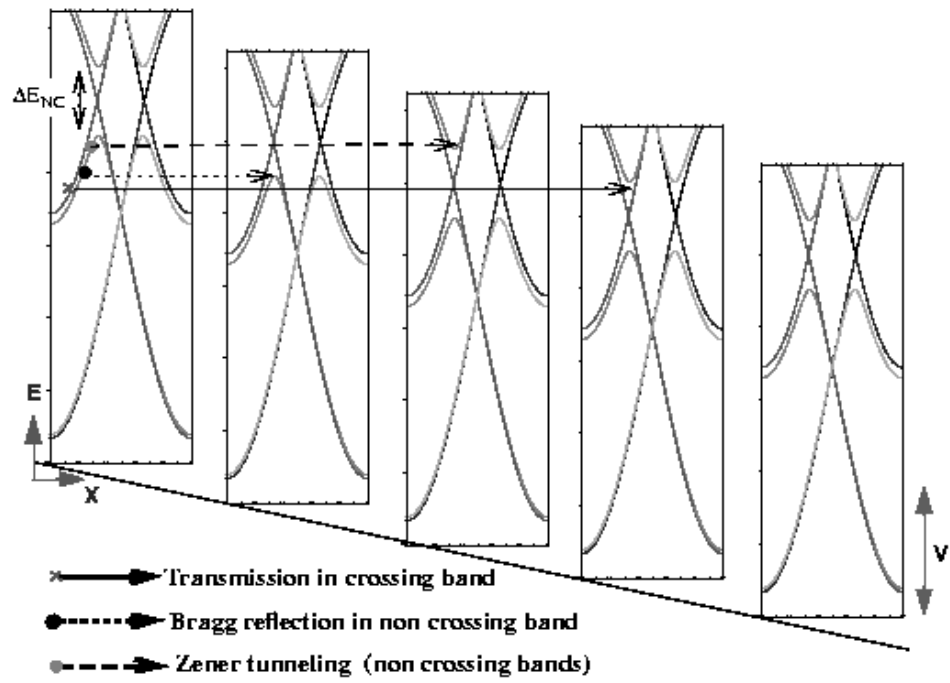


Fig 2 / Anantram

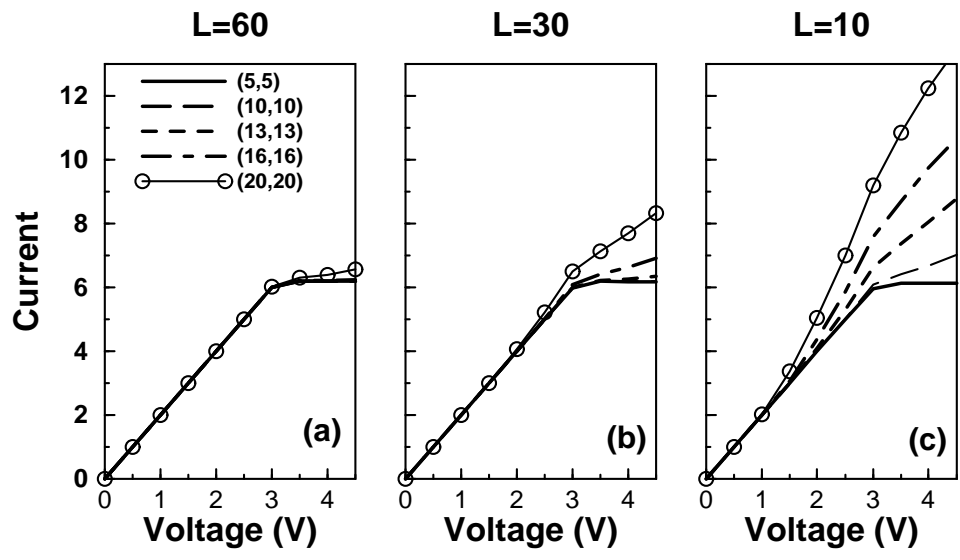


Fig 3 / Anantram

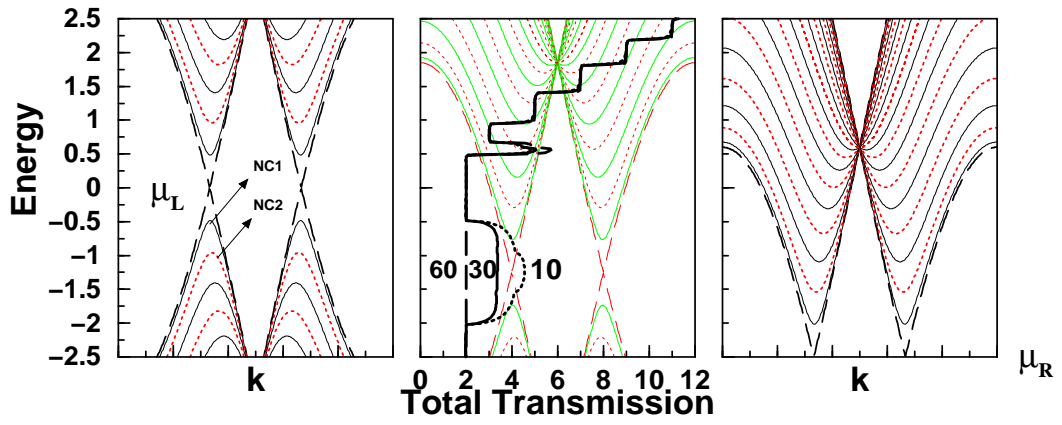


Fig 4 / Anantram

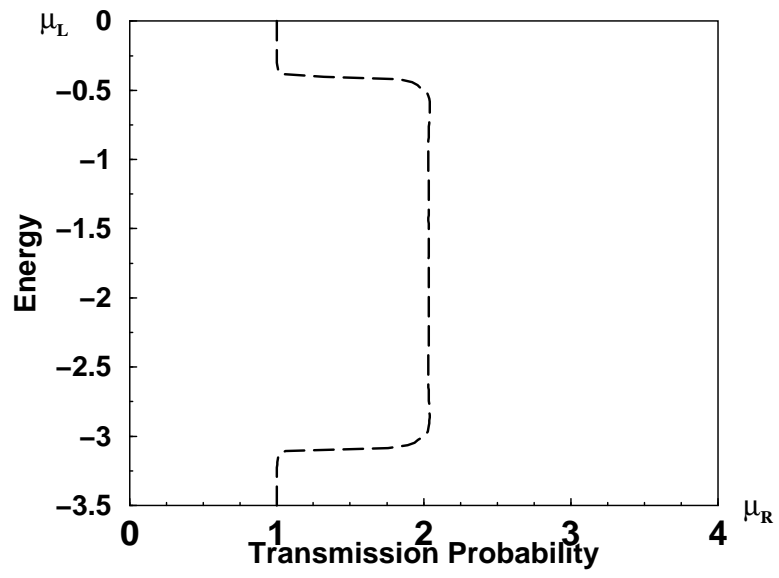


Fig. 5 / Anantram

